Time-Resolved Photodissociation of Gas-Phase Ferrocene Cation: Energetics of Fragmentation and Radiative Relaxation Rate at Near-Thermal Energies

James D. Faulk and Robert C. Dunbar*

Contribution from the Chemistry Department, Case Western Reserve University, Cleveland, Ohio 44106. *Received February 14, 1992*

Abstract: The dissociation of C_5H_5' from the molecular ion of ferrocene was induced by a short UV laser pulse and followed by time-resolved photodissociation (TRPD) techniques in the ion cyclotron resonance spectrometer. The dissociation rate was measured for two-photon absorption at 355 nm (7.8×10^4 s^{-1} at 7.24 eV of internal energy), and an upper limit was established for one-photon absorption at 240 nm (<50 s^{-1} at 5.42 eV of internal energy). A range of acceptable rate–energy curves were fitted to these data using RRKM modeling. Within the validity of the various assumptions of this RRKM fitting procedure, an indirect assignment of 3.7 ± 0.3 eV could be made for the activation energy for ring–metal bond cleavage. This value is a useful estimate of the ring–metal bond strength in the ion and is in good accord with expectations from the previously known average bond strengths in the neutral species and the ion. Using the TRPD rate as a thermometric probe of ion internal energy, the cooling of initially hot ferrocene ions was measured over a cooling range from 0.7 to 0.24 eV of internal energy, and a rate constant for infrared-radiative energy loss of 0.28 ± 0.08 s^{-1} was obtained. This constitutes the slowest radiative cooling rate constant so far observed for a polyatomic ion in our laboratory.

Introduction

Several new experimental methods which observe ion fragmentation kinetics with well-resolved internal energy have greatly advanced our knowledge of gas-phase ion properties. In addition to the time-resolved photodissociation (TRPD) approach used in the present study,[1-9] the technique of photoelectron photoion coincidence (PEPICO) has been extensively applied,[10] principally to ions of organic molecules, and dissociative multiphoton ionization (MPI) has been used in a few cases with impressive success.[11,12] In contrast to the wealth of quantitative information now known for organic ions, far less is known quantitatively about organometallic ions. It seemed of particular interest to apply an energy-resolved technique to ferrocene, a prototypical organometallic, in search of a new quantitative understanding of its properties. This work follows naturally our previous investigation of the ferrocene ion by photodissociation spectroscopy,[13] which aimed at elucidating its gas-phase spectroscopic properties.

In the present experiments, we set out to measure two properties of the ferrocene ion which have been essentially unknown. The first was the metal–ring bond strength, i.e., the energy required to remove one cyclopentadienyl ring (C_5H_5', designated as Cp in the following) from the molecular ion. The second was the radiative relaxation rate for cooling of the ion by emission of infrared photons.

The only information which appears to exist for the metal–ring bond strength comes[14,15] from ionization energy measurements of the parent $Fe(Cp)_2^+$ ion (6.75 eV) and appearance energy measurements of the fragment $Fe(Cp)^+$ ion (12.8–13.8 eV). The difference between these energies would suggest an endothermicity of 6–7 eV for the dissociation

$$Fe(Cp)_2^+ \rightarrow Fe(Cp)^+ + Cp \qquad (1)$$

This is an unrealistically high energy for the metal–ring binding, and clearly, as is amply confirmed by the discussion below, the appearance energy measurements for $Fe(Cp)^+$ were affected by a very large kinetic shift. The value derived from these prior determinations is at best an upper limit, and the bond strength is not an experimentally well-known quantity.

The rate of cooling of a number of collision-free organic ions by infrared emission has been measured in our laboratory, but nothing is known about this process for any metal-containing species. Moreover, the IR-radiative cooling rate has been reported[16] for only one other ion (the ion of *n*-butylbenzene) with a vibrational heat capacity comparably large to that of ferrocene. Thus this ion explores new territory in the field of radiative cooling.

Radiative cooling has been studied in two fairly distinct regimes of internal energy. Two-photon kinetics techniques have given cooling rates for a variety of ions with rather high internal energies in the 2–4 eV range,[17-24] while ion thermometry techniques (branching ratio determinations[16,25] and TRPD determinations[1,3]) have given cooling rates for ions with low internal energies of the order of 0.5 eV. As expected, the more energetic regime tends to give substantially higher cooling rates, with 5–10 s^{-1} being a typical cooling rate constant. In the low-energy regime ion thermometry by branching ratios yielded cooling rate constants of 1 s^{-1} for the dioxane ion[25] and 0.5 s^{-1} for the *n*-butylbenzene[16] ion. Ion thermometry by TRPD has given cooling rate constants of 0.4 s^{-1} for the chlorobenzene ion[1] and 0.65 s^{-1} for the styrene ion.[3]

It is somewhat uncertain how the ferrocene ion, containing ~0.5 eV of excess internal energy, will compare with these known

* Author to whom correspondence should be addressed.

(1) Dunbar, R. C. *J. Phys. Chem.* **1987**, *91*, 2801.
(2) So, H. Y.; Dunbar, R. C. *J. Am. Chem. Soc.* **1988**, *110*, 3080.
(3) Dunbar, R. C. *J. Chem. Phys.* **1989**, *91*, 6080.
(4) Dunbar, R. C. *J. Phys. Chem.* **1990**, *94*, 3283.
(5) Faulk, J. D.; Dunbar, R. C.; Lifshitz, C. *J. Am. Chem. Soc.* **1990**, *112*, 7893.
(6) Dunbar, R. C.; Lifshitz, C. *J. Chem. Phys.* **1991**, *94*, 3542.
(7) Huang, F. S.; Dunbar, R. C. *J. Am. Chem. Soc.* **1990**, *112*, 8167.
(8) Huang, F. S.; Dunbar, R. C. *Int. J. Mass Spectrom. Ion Processes* **1991**, *109*, 151.
(9) Faulk, J. D.; Dunbar, R. C. *J. Phys. Chem.* **1991**, *95*, 6932.
(10) See, for instance: Baer, T. *Adv. Chem. Phys.* **1986**, *LXIV*, 111.
(11) Syage, J. A.; Wessel, J. E. *Appl. Spectrosc. Rev.* **1988**, *49*, 1.
(12) Neusser, H. J. *J. Phys. Chem.* **1989**, *93*, 3897.
(13) Faulk, J. D.; Dunbar, R. C. *J. Am. Soc. Mass Spectrom.* **1991**, *2*, 97.
(14) Rosenstock, H. M.; Draxl, K.; Steiner, B. W.; Herron, J. T. *J. Phys. Chem. Ref. Data* **1977**, *6*, Suppl. 1.
(15) Lias, S. G.; Bartmess, J. E.; Liebman, J. F.; Holmes, J. L.; Levin, R. D.; Mallard, W. G. *J. Phys. Chem. Ref. Data* **1988**, *17*, Suppl. 1.
(16) Uechi, G. T.; Dunbar, R. C. *J. Chem. Phys.* **1990**, *93*, 1626.
(17) Honovich, J. P.; Dunbar, R. C. *J. Am. Chem. Soc.* **1982**, *104*, 6220.
(18) Dunbar, R. C.; Chen, J.-H. *J. Phys. Chem.* **1984**, *88*, 1401.
(19) Honovich, J. P.; Dunbar, R. C.; Lehman, T. *J. Phys. Chem.* **1985**, *89*, 2513.
(20) Dunbar, R. C. *Chem. Phys. Lett.* **1986**, *125*, 543.
(21) Dunbar, R. C.; Chen, J. H.; So, H. Y.; Asamoto, B. *J. Chem. Phys.* **1987**, *86*, 2081.
(22) Asamoto, B.; Dunbar, R. C. *J. Phys. Chem.* **1987**, *91*, 2804.
(23) Asamoto, B.; Dunbar, R. C. *Chem. Phys. Lett.* **1987**, *139*, 225.
(24) Ahmed, M. S.; So, H. Y.; Dunbar, R. C. *Chem. Phys. Lett.* **1988**, *151*, 128.
(25) Huang, F. S.; Dunbar, R. C. *J. Am. Chem. Soc.* **1989**, *111*, 6497.

0002-7863/92/1514-8596$03.00/0

organic ions in its cooling rate. The presence of a number of low-frequency vibrational modes associated with the metal should be favorable for infrared radiative cooling:[26] At 500 K, which is the temperature region of interest here, ferrocene has strongly IR-active modes[27] at 170, 480, and 496 cm^{-1} which have large $v = 1$ populations. There are also strongly allowed modes at 816, 1012, and 1112 cm^{-1} which, while largely frozen out, may still make noticeable contributions to radiative cooling. On the other hand, the high heat capacity of the molecule leads to low internal temperatures, which is unfavorable to infrared radiative emission;[26] for a given amount of excess internal energy this will tend to make ferrocene a slower-cooling molecule than smaller molecules like the molecules with 12–14 atoms which we have studied. Experiment is clearly needed to assess the balance of these competing factors.

Experimental Section

The work presented here was carried out on an ion cyclotron resonance (ICR) mass spectrometer equipped with phase-sensitive detection which has been described elsewhere.[1-6] The TRPD experiment has been described in detail in previous publications.[1-9] Briefly, ions formed by electron impact from ferrocene vapor were trapped in the ICR ion trap and photoexcited by a short laser pulse; their subsequent dissociation into fragments was followed as a function of time using the detection capability of the ICR spectrometer.

Ionization was by an electron beam pulse of about 70-ms duration at a nominal electron energy of 12 eV. Before photoexcitation by the laser pulse, parent ions were allowed to cool using various combinations of cooling time and pressure of neutral ferrocene collision gas. Following photoexcitation by the laser pulse, a variable delay time (1 μs to 100 ms) was used to allow dissociation to proceed, following which an excitation pulse of 20-μs duration and 50 V_{pp} was applied at the frequency of the $Fe(C_5H_5)^+$ photoproduct. The photoproduct was then detected by a 3-ms transient acquisition. The magnetic field was 1.4 T. Ferrocene pressure was measured with an ionization gauge, which was expected to be reliable in giving relative pressures. For absolute pressure assignment, a gauge correction factor of 7.1 was applied on the basis of the number of electrons in ferrocene,[28] but this is an extremely approximate correction and the absolute pressure of ferrocene should be regarded as highly uncertain.

A small amount of the $Fe(Cp)^+$ fragment was formed in the electron impact ionization and decayed away rapidly (probably by charge transfer to neutral ferrocene). In experiments where the laser pulse was delivered while this ion was still present, the possibility existed that the results could be distorted by photodissociation of this preexisting fragment ion. However, the signal observed for the photoinduced $Fe(Cp)^+$ fragment at 355 nm was independent of whether the electron-impact-produced fragment was present or absent, ruling out this possible artifact. When it was present, the electron-impact-produced fragment gave a constant additive contribution to the $Fe(Cp)^+$ peak, which was subtracted from the peak heights before analysis. No electron-impact- or photoproduced Fe^+ fragment was observed.

Parent ions were irradiated with a 10-ns, 355-nm laser pulse generated by tripling the fundamental of a Lumonics HY1200 pulsed YAG laser. The beam was circular in cross-section and had a diameter of about 1 cm. The generation of the 240-nm laser pulse by doubling of 480-nm light from the dye laser has been described.[13] Typical pulse energies were 15 mJ at 355 nm and 0.5 mJ at 240 nm.

Results

The ferrocene cation underwent photofragmentation at UV wavelengths according to eq 1. The progress of this process was followed by monitoring the appearance of the $Fe(Cp)^+$ photoproduct ion after the laser shot.

At 355 nm the dissociation proceeds by a two-photon mechanism which pools the energy (7.0 eV) of two photons (along with any preexisting thermal internal energy) in the internal degrees of freedom. Fortunately, the dissociation rate at this energy lies in the range measurable by our TRPD experiment, and measurements at this wavelength constitute the principle results of this work. The shortest wavelength at which we could generate sufficient light intensity to observe any dissociation was 240 nm (5.2 eV). At 240 nm, two-photon dissociation (10.3 eV of energy) is expected to be much too fast for time resolution, but we hoped that a time-resolvable component of slow one-photon (5.2 eV) dissociation could be observed on top of the fast two-photon component. This was not observed, apparently because dissociation at this energy is too slow. Considerable effort was made to generate sufficient light at another time-resolvable wavelength, either by one-photon dissociation at a wavelength shorter than 240 nm or by two-photon dissociation at a wavelength longer than 355 nm, but this was not successful.

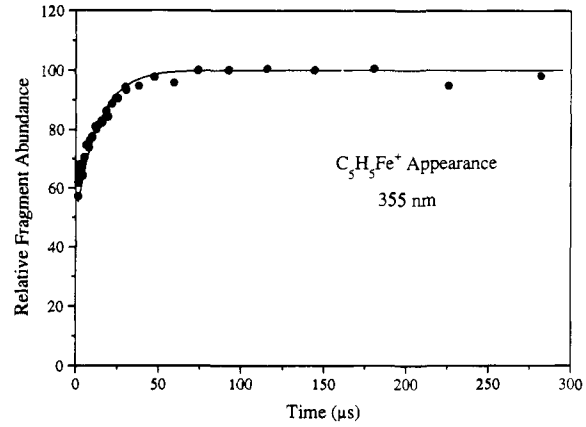

Figure 1. Time-resolved appearance curve of $Fe(C_5H_5')^+$ from the thermalized ferrocene cation at 355 nm. Solid line is the exponential fit to the data with a rate constant of 7.5×10^4 s^{-1}.

Table I. Experimental Rate–Energy Data Points

wavelength (nm)	total internal energy[a] (eV)	fragmentation rate (s^{-1})
240	5.42	<50
355	7.24	7.8×10^4

[a] Includes the energy of the photon and 0.24 eV of thermal energy.

Dissociation Rate versus Internal Energy. Time-resolved appearance curves of thermalized parent ions at 355 nm showed apparently exponential time dependence, as illustrated in Figure 1. As has been discussed,[4a] the TRPD curve for a thermal ion population deviates in general from exponential decay, but the deviation is very slight if the thermal internal energy is small compared with the internal energy of the photoexcited ion. Since the average thermal energy in this case (0.24 eV) is indeed small compared with the total internal energy (7.24 eV), the exponential approximation was expected to be excellent. The experimental curves were fitted to a single exponential, assuming all fragmenting ions had absorbed two photons, and the unimolecular dissociation rate was assigned as the inverse time constant of the fitted curve.

The appearance rate was found to depend on the extent to which the ion population had been thermalized. Rates varied from $(7.8 \pm 2) \times 10^4$ s^{-1} for thermalized ions to greater than 3×10^5 s^{-1} for the most vibrationally hot ions. For measurement of the rate constant for thermalized ions, cooling times of the order of 2.5 s at 5×10^{-7} Torr were used, which is more than sufficient, on the basis of the analysis of cooling kinetics described below, to equilibrate the ions to the ambient cell temperature (assumed to be 375 K).

In ref 13 the fragmentation rate of ions having 5.42 eV of internal energy (one 240-nm photon plus 0.24 eV of thermal energy) was reported to be less than 500 s^{-1}, based on the absence of a slow time-resolved component on top of the observed fast two-photon dissociation. Further examination of those data has allowed us to push this limit to less than 50 s^{-1}.

These results for the dissociation rate versus internal energy are summarized in Table I and plotted in Figure 2.

Thermochemical Information. When two or more points on the rate–energy curve are available for an ion dissociation reaction, it is often possible, using RRKM modeling of the dissociation process, to derive an accurate value for the critical energy of dissociation.[4] This is most conveniently done by fitting the kinetic parameters E_0 (the critical energy) and ΔS^*_{1000} (the entropy of

(26) Dunbar, R. C. *J. Chem. Phys.* **1989**, *90*, 7369.
(27) Lippincott, E. R.; Nelson, R. D. *J. Am. Chem. Soc.* **1956**, *77*, 4990; *Spectrochim. Acta* **1958**, *10*, 307.
(28) Bartmess, J. E.; Georgiadis, R. M. *Vacuum* **1983**, *33*, 149.

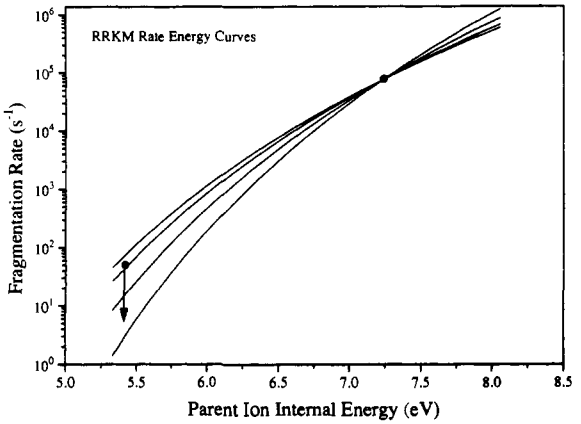

Figure 2. Experimental rate–energy points at 5.42 and 7.24 eV and four RRKM theory rate–energy curves: (1) $\Delta S^{\ddagger}_{1000}$ = 0.9 cal/K, E_0 = 3.40 eV; (2) $\Delta S^{\ddagger}_{1000}$ = 3.0 cal/K, E_0 = 3.52 eV; (3) $\Delta S^{\ddagger}_{1000}$ = 7.14 cal/K, E_0 = 3.75 eV; and (4) $\Delta S^{\ddagger}_{1000}$ = 12.7 cal/K, E_0 = 4.04 eV.

Table II. Rate–Energy Curves (from RRKM Modeling) Consistent with the Experimental Rate–Energy Data

curve no.	rate at 5.42 eV (s^{-1})	$\Delta S^{\ddagger}_{1000}$ (cal/K)	E_0 (eV)
1	74	0.90	3.40
2	45	3.0	3.52
3	15	7.14	3.75
4	3	12.66	4.05

activation at 1000 K) to the experimental points through the RRKM calculation and taking E_0 as a measure of the activation energy. (The dissociation energy may not be the same as E_0 as, for instance, happens when there is a rearrangement transition state or a significant reverse activation barrier. The present case, which to all appearances is a simple dissociation, is one where E_0 can probably be taken as a good approximation of the dissociation endothermicity.)

Analysis of the present results was less simple because only one point (355 nm) on the rate–energy curve was actually measured, together with the upper limit, determined at 240 nm. Accordingly, a family of possible rate–energy curves can be drawn consistent with the data. All of the curves must pass through the measured 355-nm point; the slopes of the acceptable curves are limited at one extreme by the limiting rate value at 240 nm and at the other extreme by consideration of the loosest transition state (largest $\Delta S^{\ddagger}_{1000}$) which we consider reasonable for the dissociation process.

RRKM calculations of the dissociation rate–energy curves were carried out using neutral ferrocene vibrational frequencies[27] for the activated molecule. For the transition states, one mode of 482 cm^{-1} was deleted from this frequency set to represent the reaction coordinate, and the frequencies of several other modes were varied to increase or decrease the looseness of the transition state. It is widely accepted that the details of the frequency changes used in the transition state are not very important;[29] what is important is the resulting tightness or looseness of the transition state, which is usefully characterized by the single parameter $\Delta S^{\ddagger}_{1000}$.

The family of acceptable fitted curves is shown in Figure 2, where four curves are drawn which are consistent with the requirements that they pass through the point at 7.24 eV (two 355-nm photons) and through or below the point at 5.42 eV (one 240-nm photon). The activation parameters corresponding to this family of curves are shown in Table II. The curve of lowest slope (curve 1) represents the tightest allowable transition state, as imposed by the upper-limit point at 240 nm; its $\Delta S^{\ddagger}_{1000}$ of 0.9 eu is lower than would be expected for a simple ionic bond stretching dissociation. The curve of highest slope (curve 4) was drawn using a $\Delta S^{\ddagger}_{1000}$ of 12.7 eu, which was taken as a conservative estimate of the loosest plausible transition state. This can be compared with values collected by Lifshitz[29] for the $\Delta S^{\ddagger}_{1000}$ values of several simple bond cleavage dissociations of ions, found to be in the range of 7–10 eu. No simple bond cleavage dissociation of an ion has been reported with a $\Delta S^{\ddagger}_{1000}$ as large as 12 eu. This analysis then leads to lower and upper limits on E_0, as listed in Table II, of 3.4 and 4.0 eV. We thus arrive at a confident assignment of E_0 = 3.7 ± 0.3 eV.

(29) Lifshitz, C. *Adv. Mass Spectrom.* **1989**, *11*, 113.

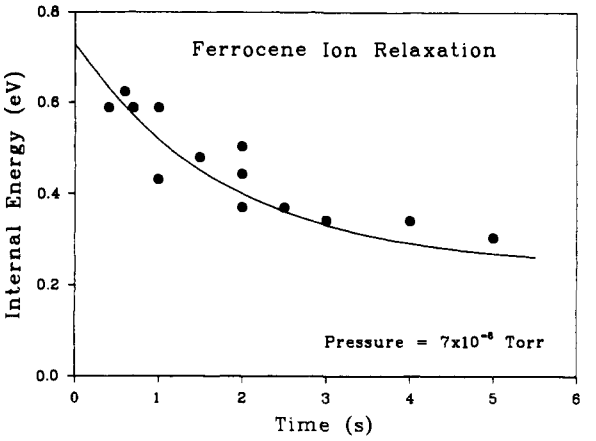

Figure 3. Decay of parent ion internal energy with increasing cooling time at a constant pressure of 7 × 10^{-8} Torr (indicated). Circles are experimental points and the solid curve is a calculated exponential decay curve derived using least-squares fit parameters from Table IV.

Table III. Cooling Data for Electron-Impact-Generated Ferrocene Ion

pressure[a] (10^{-8} Torr)	cooling time (s)	energy[b] (eV)	dissociation rate (10^5 s^{-1})
1	2.0	0.59, 0.63	2.0, 2.3[c]
	3.0	0.40	1.2
	4.0	0.26	0.8
	5.0	0.26	0.8
7	0.4	0.59	2.0
	0.6	0.62	2.2
	0.7	0.59	2.0
	1.0	0.59, 0.43	2.0, 1.3
	1.5	0.48	1.5
	2.0	0.50, 0.44, 0.37	1.6, 1.4, 1.1
	2.5	0.37	1.1
	3.0	0.34, 0.34	1.0, 1.0
	4.0	0.34	1.0
	5.0	0.30	0.9
10	0.4	0.57	1.9
	0.5	0.61	2.1
	1.0	0.48	0.8
	1.5	0.40	1.2
	2.0	0.40	1.2
	3.0	0.30	0.9
	3.9	0.34	1.0
50	1.0	0.26	0.8[d]
	1.9	0.17	0.6[e]
	2.3	0.24	0.75[e]
	2.5	0.24	0.75[f]
	3.0	0.26	0.8

[a] Pressures indicated by the ionization gauge, without correction by the gauge calibration factor. [b] Rate–energy curve 2 was used to convert observed dissociation rates into ion internal energies. [c] 8 × 10^{-9} Torr. [d] 5.2 × 10^{-7} Torr. [e] 4.5 × 10^{-7} Torr. [f] 5.5 × 10^{-7} Torr.

Cooling of Ferrocene Cation. Since the fragmentation rate at 355 nm is dependent on the internal energy of the ion before photon absorption, measurement of this rate can be used in a thermometric sense as a convenient way of monitoring the ion's internal energy as a function of time. The conversion of the measured dissociation rate to ion internal energy (the thermometric calibration) is done using one of the rate–energy curves derived above. Since the ions are formed by electron impact with substantial excess internal energy, the cooling of the initially hot ion can be measured directly.

Using the unimolecular fragmentation rate as a probe in this way, the ion's internal energy at the end of the cooling time period

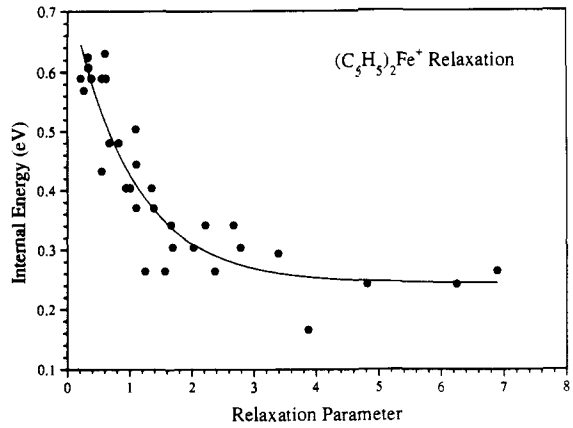

Figure 4. Parent ion internal energy versus extent of thermalization. The internal energy is measured as described in the text using curve 2 for the thermometric calibration. The extent of cooling is parametrized by the relaxation parameter, $(k_r + k_c p)t$, where t is the cooling time between the electron beam pulse and the YAG laser probe pulse. This is the full data set which includes the points plotted in Figure 3 as well as points at other pressures. Experimental points (●); exponential fit (—).

was measured for 33 combinations of neutral pressures p (8×10^{-9} to 5×10^{-7} Torr indicated) and cooling times t (0.4–5 s). The measured rates were converted to internal energies using each of the four rate–energy curves in Figure 2. For illustration, Figures 3 and 4 and Table III show results calibrated using the rate–energy curve denoted curve 2 in Figure 2. The cooling curves derived from the four different calibrations differed somewhat in the initial energy E_{in} derived for the ferrocene ion, but the cooling rate constants were essentially independent of which calibration was used.

Table III shows the data set for the cooling of the ferrocene ion. Figure 3 illustrates the decay of ion internal energy with cooling time at one particular pressure, 7×10^{-8} Torr; at this pressure the radiative and collisional relaxation contributions are roughly equal. The group of low-pressure pressure points at 1×10^{-8} Torr (for which collisional relaxation was negligible) shows at once that the radiative relaxation time constant is of the order of 3 s. Figure 4 displays the entire set of relaxation data as a function of the relaxation parameter defined below.

In deriving the cooling rate constants from the observed cooling curve, it was assumed that the internal energy decreased exponentially due to both collisional and radiative processes according to

$$E(p,t) = (E_{in} - E_{th}) \exp[-(k_r + k_c p)t] + E_{th} \qquad (2)$$

where E_{in} is the initial internal energy from electron impact, E_{th} is the final thermal energy, k_c and k_r are the rate constants for the collisional and radiative relaxation processes, respectively, p is the pressure of neutral ferrocene, and t is the time interval between the electron beam pulse and the laser pulse. If we define a "relaxation parameter" as $(k_r + k_c p)t$, a plot of internal energy versus relaxation parameter, as in Figure 4, should fall exponentially with decay constant $(k_r + k_c p)$, from which the radiative and collisional cooling rate constants can be extracted.

The most reliable method for extracting k_r and k_c was a nonlinear least-squares fit of eq 2 to the entire data set in which E_{in}, E_{th}, k_c, and k_r were considered to be adjustable parameters. The data showed substantial scatter around the best-fit curve, mainly attributable to the rather weak dependence of dissociation rate on internal energy, which magnified the uncertainties in the dissociation rate measurements. The rms deviation of internal energies from the curve was of the order of 0.05 eV. The deviations appeared to be random, and it seemed justifiable to assign an uncertainty to our determination of k_r using statistical methods.[30] For the fit using calibration number 2, a χ^2 map in the fitting parameter space was calculated around the minimum, and the uncertainties (1 standard deviation) in k_r and k_c were estimated from the χ^2 variation. The values obtained from the fits are shown in Table IV and lead to the final values $k_r = 0.28 \pm 0.08$ s^{-1}, $k_c = (9 \pm 3) \times 10^{-10}$ cm^3 molecule^{-1} s^{-1}, $E_{in} = 0.70 \pm 0.07$ eV, and $E_{th} = 0.24$ eV. The exponential decay expected from eq 2 is displayed with the corresponding data in Figures 3 and 4.

(30) Bevington, P. R. *Data Reduction and Error Analysis for the Physical Sciences*; McGraw-Hill: New York, 1969.

Table IV. Fits of the Cooling Parameters to the Cooling Data Using Four Thermometric Calibration Curves from Table II

curve no.	E_{th} (eV)	E_{in} (eV)	k_r (s^{-1})	k_c (cm^3 molecule^{-1} s^{-1})	$\Delta S^{\ddagger}_{1000}$ (cal/K)	E_0 (eV)
1	0.254	0.78	0.284	9.1×10^{-10}	0.90	3.40
2	0.244	0.74	0.274	8.5×10^{-10}	3.0	3.52
3	0.254	0.69	0.28	9.1×10^{-10}	7.14	3.75
4	0.254	0.61	0.27	8.5×10^{-10}	12.7	4.05

Because of the relatively low vapor pressure of ferrocene, the separation between the ICR cell and the ionization gauge, and the fact that the ionization gauge was not experimentally calibrated for ferrocene, the absolute pressure inside the ICR cell was very uncertain. Because of this uncertainty the fitted value for k_c is at best a rough estimate of the actual collisional cooling rate constant (much more uncertain than the statistical uncertainty given above). However, the value for the IR-radiative cooling rate constant k_r is independent of the pressure calibration as well as of the thermometric calibration and is considered a firm number within the indicated statistical uncertainty. The greatest systematic uncertainty in k_r is probably the uncorrected collisional cooling due to background gas in the cell. Given a base pressure of about 5×10^{-9} Torr and assuming 10% energy removal per collision with a background gas molecule, we would guess that this contributes a systematic error of the order of 0.02 s^{-1} or less to k_r.

Discussion

Ferrocene Bond Strengths. These results give for the first time a useful determination of the strength of the metal–ring bond in the ferrocene ion. Some context for interpreting this number comes from the energy of disassembling neutral ferrocene which is accurately known from heat of formation data[14,15]

$$Fe(Cp)_2 \rightarrow Fe + 2Cp \qquad \Delta H = 656 \text{ kJ/mol} \qquad (3)$$

and for disassembling the ferrocene ion

$$Fe(Cp)_2^+ \rightarrow Fe^+ + 2Cp \qquad \Delta H = 764 \text{ kJ/mol} \qquad (4)$$

Simply by dividing these numbers by 2, we can write an average ring–metal bond strength of 328 kJ/mol (3.42 eV) for the neutral ferrocene and 382 kJ/mol (3.98 eV) for the ion.

These average bond strengths come from well-established thermochemistry. One useful aspect of this calculation is that it leads to some assurance that the slow ion dissociation observed at 355 nm is exactly two-photon and not one-photon or three-photon. The average ion bond strength of 3.98 eV must give at least a first approximation to the dissociation energy of reaction 1. Assuming some degree of validity for an RRKM description of the dissociation and a critical energy in the vicinity of 4 eV, it is impossible for dissociation with 3.7 eV of internal energy (one photon plus thermal) to be as fast as observed, while dissociation with 10.7 eV (three photons) would be in accord with our result only with an activation energy around 5 eV.

The possibility that the observed time-resolved dissociation at 355 nm is three-photon needs further consideration. The strongest argument for ruling it out is that if this were the case we would have observed time-resolved dissociation from two photons at 240 nm (10.6 eV) with a rate not much different from that of three photons at 355 nm (10.7 eV), which we did not. An additional argument is that if the activation energy were higher than 5 eV we would calculate the kinetic shift to be so large that the electron impact appearance potential for $Fe(Cp)^+$ would be at least 1 eV

higher than the highest literature value.

In the context of the average ion bond strength of 3.98 eV, the value of 3.7 eV assigned here as the endothermicity of the first dissociation (eq 1), seems entirely reasonable as an order of magnitude. We may go further and try to understand why the energy of the first dissociation of the ion, determined here to be 3.7 eV, can be less than that of the second dissociation

$$Fe(Cp)^+ \rightarrow Fe^+ + Cp \qquad (5)$$

which must be 4.3 eV by subtraction. Ion solvation effects can account for this difference and explain the fact that the average bond energy is larger in the ion than in the neutral species. The argument is that the electronic aspects of the ring–metal bonding are probably similar for the different cases but that an additional degree of stabilization (a solvation energy) is gained from electrostatic forces when a Cp ring attaches to a gas-phase ion. The greatest solvation energy will be expected when the bare metal ion is solvated, as in eq 5; thus the dissociation energy of eq 5 should be exceptionally large. An additional but smaller stabilization will be expected in eq 1 from the solvation of the $Fe^+(Cp)$ ion by the second Cp ring, so we expect the endothermicity of eq 1 to be less than that of eq 5 but greater than the metal–ring bond strength in the neutral ferrocene which gains nothing from charge solvation stabilization. These predictions are exactly in line with what is observed.

Since the heats of formation of the other species in eq 1 are known, the present assignment of the energy of this reaction is equivalent to a heat of formation value for $Fe(C_5H_5)^+$. Subject to the same assumptions as were outlined for the bond strength assignment, we can assign a $\Delta H_{f\,298}$ value of 1009 ± 30 kJ mol^{-1} to $Fe(C_5H_5)^+$.

Kinetic Shift. The conventional kinetic shift can be defined[7,9] as the internal energy (in excess of the activation energy) that must be supplied to give a fragmentation rate of 1000 s^{-1} or more. It is expected to be large for ions such as this one that have a large number of vibrational modes. The rate–energy curves in Figure 2 show that the internal energy content must be at least 6 eV for the fragmentation rate to be greater than 1000 s^{-1}, corresponding to a kinetic shift of at least 2.3 eV. It is not surprising that our value for E_0 is at least 2 eV lower than the threshold of 6–7 eV based on electron impact appearance energies taken from the literature.[14,15]

Radiative Relaxation. These results represent the first attempt to measure the radiative relaxation rate of an organometallic cation in the near-thermal internal energy regime (0.25–0.75 eV). In terms of internal temperature, the range of cooling observed in these experiments was from approximately 600 to 375 K. The radiative cooling rate constant (0.28 s^{-1}) is the lowest yet measured for polyatomic ion cooling in this energy regime but is not very different from those of other slow-cooling ions, notably the *n*-butylbenzene ion[16] (0.5 s^{-1}) and the chlorobenzene ion[1] (0.4 s^{-1}). The slow observed cooling of the ferrocene ion suggests that the tendency of its relatively large heat capacity in this temperature region to depress IR-radiative cooling outweighs the IR-radiative strength of its numerous low-frequency IR-active vibrational modes.

Note Added in Proof. Prof. Amster has called to our attention a recent determination of the heat of formation of $FeCp^+$ by Huang and Freiser, uisng a very different route. (Huang, Y.; Freiser, B. S. *J. Am. Chem. Soc.* **1990**, *112*, 5085.) Their value of 1045 ± 29 kJ mol^{-1} is in gratifying agreement with our result.

Acknowledgment. Support for this research is acknowledged from the National Science Foundation and the donors of the Petroleum Research Fund, administered by the American Chemical Society.

Dicoordinated Boron Cations Dehydrate Organic Ethers in the Gas Phase

Thilini D. Ranatunga and Hilkka I. Kenttämaa*

Contribution from the Department of Chemistry, Purdue University, West Lafayette, Indiana 47907. *Received February 13, 1992*

Abstract: Condensed-phase studies of two-coordinated boron cations are limited to ions with conjugatively stabilizing substituents; the reactions of these ions are dominated by simple addition. We have investigated the gas-phase reactions of two simple, dicoordinated boron cations, $CH_3OBOCH_3^+$ and $CH_3BCH_3^+$, in a dual-cell Fourier-transform ion cyclotron resonance device. These ions are found to undergo a bimolecular reaction with no well-known precedent in the gas phase or in solution: facile abstraction of a water molecule from organic ethers (the efficiency, or k_{obsd}/k_{ADO}, is measured to be 0.5–0.8). The mechanism of the reaction was investigated by using different neutral ethers, deuterium labeling, collision-activated dissociation of the ionic reaction products and the proposed ionic intermediates, bimolecular reactions of the proposed intermediates, and generating the intermediates using independent routes. On the basis of these data, dehydration of organic ethers by the boron cations is proposed to occur via consecutive 1,2-elimination of two alkene molecules from the ether. The overall reaction is estimated to be highly exothermic.

Introduction

Two-coordinated boron cations are proposed to exist as transient intermediates in solution reactions of boranes.[1] Studies of these highly electrophilic species are hampered by a rapid recombination with solvent molecules and counterions. Consequently, solution studies have predominantly focused on ions with at least one nitrogen-containing substituent (usually an amino group) which effects good electronic shielding at the boron through π-back-bonding; in addition, the substituents are typically bulky and provide steric restriction for nucleophilic attack (see an example below).[1] Reactions of these borylium ions are dominated by simple addition.[1]

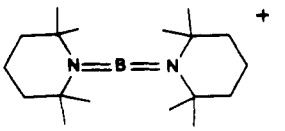

Very few gaseous dicoordinated boron cations have been studied thus far;[2-5] besides addition,[2b,3,4] only simple atom[2b] and group

(1) For recent reviews, see: (a) Nöth, H.; Rasthofer, B.; Narula, Ch.; Konstantinov, A. *Pure Appl. Chem.* **1983**, *55*, 1453. (b) Kölle, P.; Nöth, H. *Chem. Rev.* **1985**, *85*, 399.

0002-7863/92/1514-8600$03.00/0